# Acetyl-lysine Binding Site of Bromodomain-Containing Protein 4 (BRD4) Interacts with Diverse Kinase Inhibitors

Stuart W. J. Ember,[†,#] Jin-Yi Zhu,[†,#] Sanne H. Olesen,[†] Mathew P. Martin,[†] Andreas Becker,[§] Norbert Berndt,[†] Gunda I. Georg,[‡] and Ernst Schönbrunn*,[†]

[†]Drug Discovery Department and [§]Chemical Biology Core, H. Lee Moffitt Cancer Center and Research Institute, Tampa, Florida 33612, United States

[‡]Department of Medicinal Chemistry, University of Minnesota, Minneapolis, Minnesota 55455, United States

Ⓢ *Supporting Information*

**ABSTRACT:** Members of the bromodomain and extra terminal (BET) family of proteins are essential for the recognition of acetylated lysine (KAc) residues in histones and have emerged as promising drug targets in cancer, inflammation, and contraception research. In co-crystallization screening campaigns using the first bromodomain of BRD4 (BRD4-1) against kinase inhibitor libraries, we identified and characterized 14 kinase inhibitors (10 distinct chemical scaffolds) as ligands of the KAc binding site. Among these, the PLK1 inhibitor BI2536 and the JAK2 inhibitor TG101209 displayed strongest inhibitory potential against BRD4 (IC$_{50}$ = 25 nM and 130 nM, respectively) and high selectivity for BET bromodomains. Comparative structural analysis revealed markedly different binding modes of kinase hinge-binding scaffolds in the KAc binding site, suggesting that BET proteins are potential off-targets of diverse kinase inhibitors. Combined, these findings provide a new structural framework for the rational design of next-generation BET-selective and dual-activity BET-kinase inhibitors.
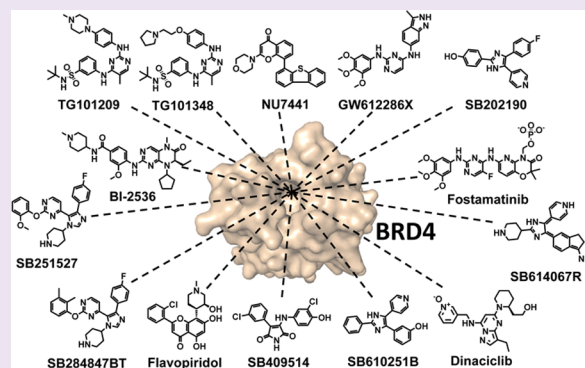
Bromodomain (BRD)-containing proteins are essential for the recognition of acetylated lysine (KAc) residues of histones during transcriptional activation.[1] An analysis of the human proteome has revealed that there are eight distinct BRD families, representing 61 different BRDs from 46 separate proteins, although others may still be undiscovered.[2] To date, crystal structures of BRDs for 43 different proteins have been published with the Protein Data Bank (PDB). These studies have provided valuable insights into structural similarities among the BRDs, including a left-handed four-helix bundle (αA, αB, αC, αZ),[1] as well as the varying loop regions (ZA and BC) that determine substrate specificity.[3] The bromodomain and extra terminal (BET) protein family (Family II) includes BRD2, BRD3, BRD4, and BRDT, each of which contains two tandem BRDs. The BRD-containing proteins have emerged as promising drug targets for a number of disease pathways that are characterized by changes in the epigenetic cell signature.[1,3] For instance, chromosomal translocation of *BRD4* to the nuclear protein in testis (*NUT*) locus generates a BRD4-NUT fusion protein that results in c-Myc overexpression and NUT midline carcinoma (NMC), an aggressive squamous cell malignancy unresponsive to conventional chemotherapeutics.[4] Direct inhibition of c-Myc by small molecules is not considered possible, and therefore the chemical inhibition of BETs holds promise as a novel therapeutic strategy to improve treatment for c-Myc-dependent cancers.[5]

BRD4 is a ubiquitously expressed protein[4] that associates with interphase chromatin and the chromosomes of mitotic and meiotic cells[6] and is currently the most extensively studied member of the BRD family, as reflected by the deposition of over 70 structures for the human isoform of this protein in the PDB. Similar to the function of other BRD-containing proteins, BRD4 is a chromatin reader protein that recognizes acetylated histones and contributes to epigenetic memory of postmitotic G1 cells by shaping transcriptional regulation across cell division.[7] Importantly, BRD4 remains associated with chromatin throughout the cell cycle, thus directly maintaining the acetylated state of histones and higher-order structure of chromatin.[8] Mechanistically, BRD4 controls signal-inducible gene transcription during interphase by recruiting the positive transcription elongation factor (P-TEFb) complex to promoters, whereupon it forms activated P-TEFb by displacing it from negative regulators, such as hexamethylene bisacetamide-inducible protein (HEXIM)1 and 7SKsnRNA.[9] Freed from inhibition, P-TEFb (which consists of cyclin-dependent kinase 9 and cyclin T1, T2, or K) phosphorylates negative elongation factors and the C-terminal domain (CTD) of RNA polymerase II (RNAPII), thereby stimulating eukaryotic transcriptional
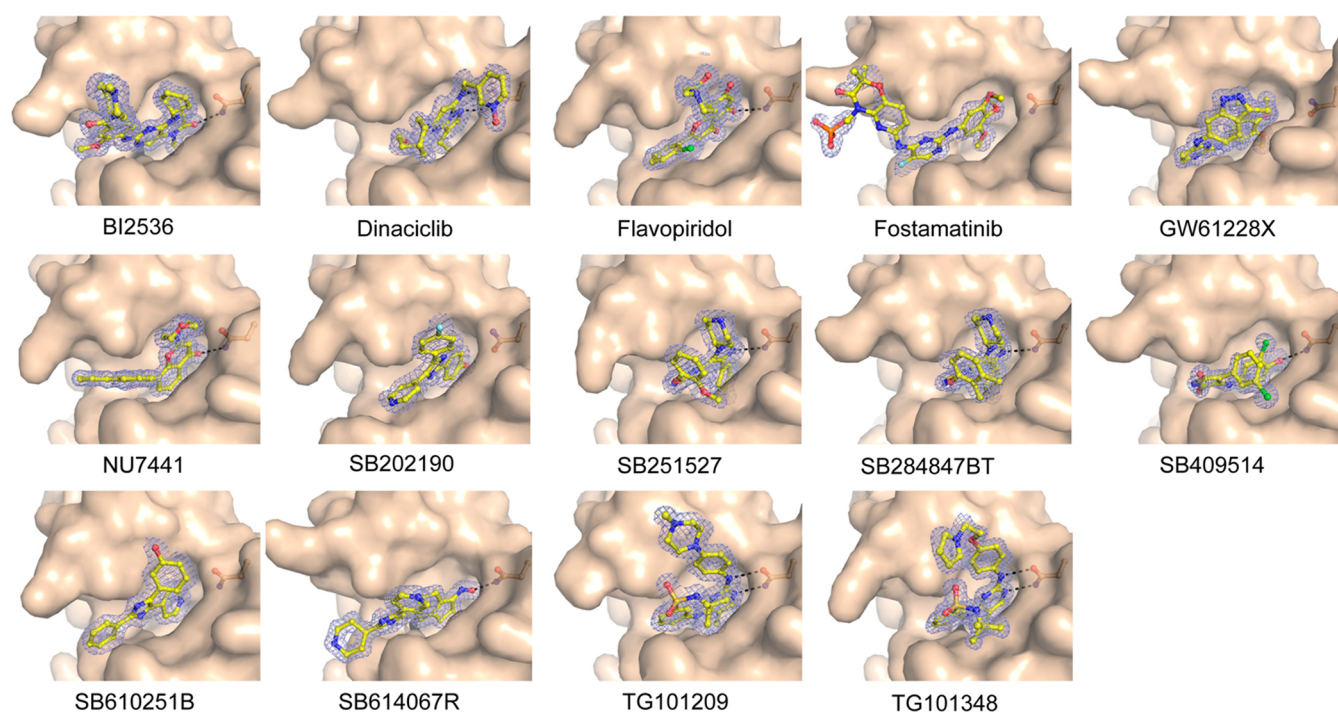
**Figure 1.** Crystal structures of BRD4-1 in complex with kinase inhibitors. Complexes were identified by co-crystallization screening against the Selleck and GSK kinase inhibitor libraries. All inhibitors bind to the KAc site of BRD4. Inhibitor is shown in yellow and the $2F_o-F_c$ electron density map (contoured at $1\sigma$) is indicated as blue mesh. $F_o-F_c$ electron density maps omitting the inhibitor during the refinement are shown in Supplementary Figure S1.

elongation. More recently, BRD4 has been demonstrated to activate transcription in a manner independent of its association with P-TEFb by recruiting nuclear SET domain-containing protein (NSD)3[10] and by directly phosphorylating Ser-2 of the CTD of RNAPII, leading to its putative characterization as an atypical kinase.[11] Furthermore, BRD4 has been implicated in NF-κB activation by recruiting P-TEFb to acetylated RELA.[12] Unlike the other BET family members, BRDT is expressed at the highest levels in meiotic prophase spermatocytes.[13] The first bromodomain of BRDT (BRDT-1) is essential for male germ cell differentiation, and homozygous knockout mice are viable but sterile,[14] making this an attractive target for the development of nonhormonal, novel male contraceptives. Similar to BRD4, BRDT interacts with P-TEFb by recruiting it to acetylated histones at the promoters of meiotic and postmeiotic genes, thereby facilitating the transcriptional changes necessary for spermatogenesis to occur.[15] Components of the mRNA splicing machinery, such as splicing factor arginine/serine-rich 2 (SFSR2), have been found to associate with BRDT in pachytene spermatocytes, and BRDT also participates in the 3′-UTR truncation of specific mRNAs in postmeiotic spermatids.[16,17] Chemical inhibition of BET proteins exerts a broad spectrum of desirable biological effects such as anticancer, anti-inflammatory, and male contraceptive properties.[17,18]

Several conserved features of the KAc site in BET BRDs are necessary for KAc binding and contribute to varying degrees for ensuring shape complementarity and optimal positioning of inhibitors. The KAc site is a hydrophobic cavity formed at one end of the BRD α-helical bundle and contains residues of the ZA and BC loops. KAc recognition is primarily mediated through a direct hydrogen bonding interaction between the acetyl carbonyl oxygen and the -NH2 group of the conserved

asparagine (Asn140 in BRD4 bromodomain 1; BRD4-1) located in the BC loop. A second indirect hydrogen bonding interaction is formed to the carbonyl oxygen of the asparagine side chain through a structurally conserved water molecule.[19] The conserved WPF shelf (Trp81-Pro82-Phe83 in BRD4-1) and KL flank (Lys82-Leu92 in BRD4-1) constitute a relatively narrow passage, which can position inhibitors through hydrophobic van der Waals (VDW) interactions. The back pocket of the KAc site is a relatively large cavity filled with water molecules, which is likely suited to accommodate small to medium sized polar or nonpolar groups, although this subsite is not utilized by known BET inhibitors. The ZA channel is mostly hydrophilic and contains an intricate network of structurally conserved water molecules and offers additional hydrogen bonding potential with small molecule inhibitors. Given the importance of the conserved asparagine in BRDs for KAc binding, it is unsurprising that the most potent BET inhibitors reported to date also target this residue for anchoring to BET BRDs. [20] Most notably, the thienodiazepine and prototypic BET inhibitor (+)-JQ1 has been successfully utilized as a chemical probe to validate BETs as therapeutic targets.[3] Importantly, inhibition of BETs by JQ1 resulted in the down-regulation of oncogenes belonging to the MYC family of transcription factors, including c-Myc, in several cancer cell lines.[18] Like JQ1, benzodiazepines such as I-BET-762 (GSK525762), which recently entered clinical trials for the treatment of NMC,[21] also contain a triazole ring which interacts with the critical Asn residue of the KAc site of BETs. Similarly, the quinoline based inhibitor I-BET-151 carries an isoxazole group that interacts with the critical Asn residue.[22] Although less potent than JQ1 or I-BET-762, I-BET-151 showed marked acceleration of apoptosis and perturbation of growth in primary cells obtained from patients with mixed

1161

dx.doi.org/10.1021/cb500072z | ACS Chem. Biol. 2014, 9, 1160−1171

lineage leukemia (MLL). Recently, a tetrahydroquinazolin-based BET inhibitor, PFI-1, was reported, which showed antiproliferative activity in leukemia cell lines arising from the induction of G1 arrest, MYC down-regulation, and apoptosis.[23] Following these promising early studies, intense research efforts are currently underway to discover new chemical scaffolds for hit-to-lead development campaigns of BET inhibitors as novel therapeutics.

In addition to their KAc recognition function, BRD-containing proteins are also considered atypical kinases,[11] but their potential to interact with kinase inhibitors was unknown until our recent discovery that the potent cyclin-dependent kinase (CDK) inhibitor dinaciclib binds to the KAc recognition site of BRDT bromodomain 1 (BRDT-1).[24] This finding led to our hypothesis that common kinase inhibitors ("hinge-binders") possess a previously unrecognized potential as inhibitors of BET proteins. Herein, we demonstrate by X-ray crystallography that the KAc site of BRD4-1 interacts with structurally diverse kinase inhibitors. Among the 14 compounds identified, the PLK1 inhibitor BI2536 and the JAK2 inhibitor TG101209 displayed nanomolar inhibitory potential against BRD4 and BRDT, and profiling against 32 human BRDs demonstrated high selectivity of these kinase inhibitors for BET proteins.

## ■ RESULTS AND DISCUSSION

Our recent finding that the CDK inhibitor dinaciclib interacts with the KAc site of BRDT suggested an intrinsic property of BETs to accommodate other kinase inhibitors, specifically, so-called hinge-binders of the Type I and II family of kinase inhibitors. To test this hypothesis, we assessed the binding potential of diverse kinase inhibitors toward BETs by robotic co-crystallization screening campaigns employing the kinase inhibitor libraries from Selleck Chemicals (277 compounds) and Glaxo Smith Kline (PKIS-I, 304 compounds).[25] Human BRD4-1 was chosen as a representative BET bromodomain as it crystallizes robustly in the presence of 10% DMSO, typically yielding highly diffracting crystals. Of the 581 compounds screened, 377 wells developed crystals within 1−3 days, most of which were of sufficient size and quality for X-ray data collection (Supplementary Table S1). The majority of droplets grew crystals with unchanged growth characteristics compared to ligand-free BRD4, although some compounds induced a change in crystal morphology and space group (Supplementary Table S2). Unliganded or JQ1-liganded BRD4 crystals in space group $P2_12_12_1$ ($a$ = 37.3, $b$ = 46.5, $c$ = 77.8) are tightly packed, and the KAc site is in close proximity to a symmetry-related BRD4 molecule. Different space groups were predominantly obtained for ligands in which a substantial portion is solvent-exposed, interfering with the packing of the symmetry-related molecule observed in unliganded or JQ1-liganded BRD4 crystals. However, there is no correlation between the inhibitor binding mode and the space group of the underlying crystal. The tight packing of BRD4 molecules around the KAc site rendered ligand-free BRD4 crystals unsuitable for in-diffusion experiments as even high affinity inhibitors such as JQ1 failed to bind at 1 mM concentration after 24 h of incubation. To this end, we determined 194 crystal structures, of which 14 structures unambiguously revealed compound bound to the KAc site of BRD4-1 (Figure 1). Thus, identified ligands were subjected to differential scanning fluorimetry (DSF) and Alpha Screen assay to assess their binding and inhibitory potentials against BRD4-1 and BRDT-1 (Figure 2A). As shown previously for other BRD-inhibitor complexes,[3] the melting temperatures

**a**

| Compound | IC$_{50}$ (μM) | | ΔT$_m$ (°C) | |
|---|---|---|---|---|
| | BRD4-1 | BRDT-1 | BRD4-1 | BRDT-1 |
| BI2536 | 0.025 | 0.26 | 9.2 | 5.2 |
| Dinaciclib | 19 | 61 | 0.59 | 1.4 |
| Flavopiridol | 18 | 91 | 0.45 | 0.98 |
| Fostamatinib | 21 | 30 | 0.12 | 0.72 |
| GW612286X | 4.6 | 7.6 | 2.5 | 3.2 |
| JQ1 | 0.035 | 0.11 | 10 | 7.0 |
| NU7441[a] | 1.0 | 3.5 | n.d. | n.d. |
| SB202190 | 2.5 | 20 | 3.4 | 5.1 |
| SB251527 | 13 | 72 | 0.64 | 0.65 |
| SB284847-BT | 20 | 44 | 0.55 | 0.05 |
| SB409514 | 19 | 13 | 0.78 | 2.2 |
| SB610251-B | 5.7 | 16 | 2.7 | 2.2 |
| SB614067-R | 10 | 92 | 0.85 | 0.79 |
| TG101209 | 0.13 | 0.23 | 7.4 | 6.2 |
| TG101348 | 0.29 | 0.34 | 7.3 | 7.0 |

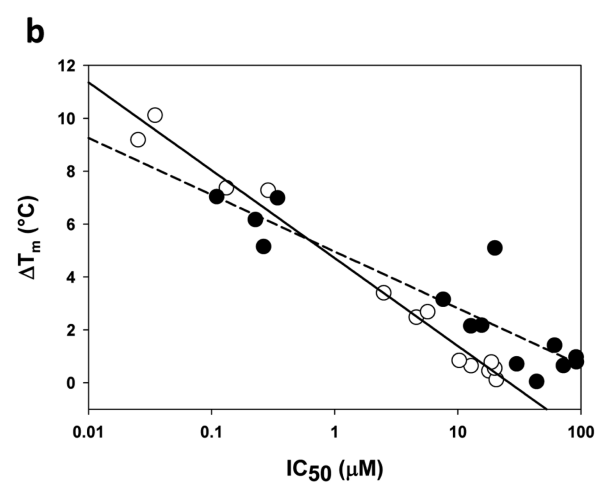[a] Not amenable to DSF due to high intrinsic compound fluorescence

**b**



**Figure 2.** Inhibitory activity and binding potential of identified kinase inhibitors against BRD4-1 and BRDT-1. (A) IC$_{50}$ values were determined by Alpha Screen assay and differential melting temperatures (ΔT$_m$) by DSF as described under Methods. Compound JQ1 served as a positive control. Dose−response graphs are shown in Supplementary Figures S2, S3. (B) Logarithmic relationship between inhibitory potency and stability of the protein-inhibitor complex for BRD4-1 (○) and BRDT-1 (●). Data were fit to $y = y_0 + a(\ln x)$ (solid and dashed lines for BRD4 and BRDT, respectively).

of BRD4-kinase inhibitor complexes were logarithmically proportional to their IC$_{50}$ values (Figure 2B).

**Binding Modes of Kinase Inhibitors in BRD4-1.** Of the compounds identified to date, BI2536 (Selleck library) was the most potent BET inhibitor with IC$_{50}$ values of 25 and 260 nM against BRD4-1 and BRDT-1, respectively. Therefore, this compound was as potent against BRD4 as the prototypic BET inhibitor JQ1, which served as a positive control in this study (Figure 2). BI2536 was developed as a potent and selective inhibitor of PLK1 (IC$_{50}$, 0.83 nM)[26] and has shown antitumor activity against relapsed or refractory acute myeloid lymphoma (AML)[27] and nonsmall-cell lung cancer in phase I/II clinical trials.[28] BI2536 binds to the KAc site of BRD4 through an elaborate network of hydrogen bonding and VDW (hydrophobic) interactions (Figure 3A). Main hydrogen bonding interactions are established through the 2-amino-6-oxo-
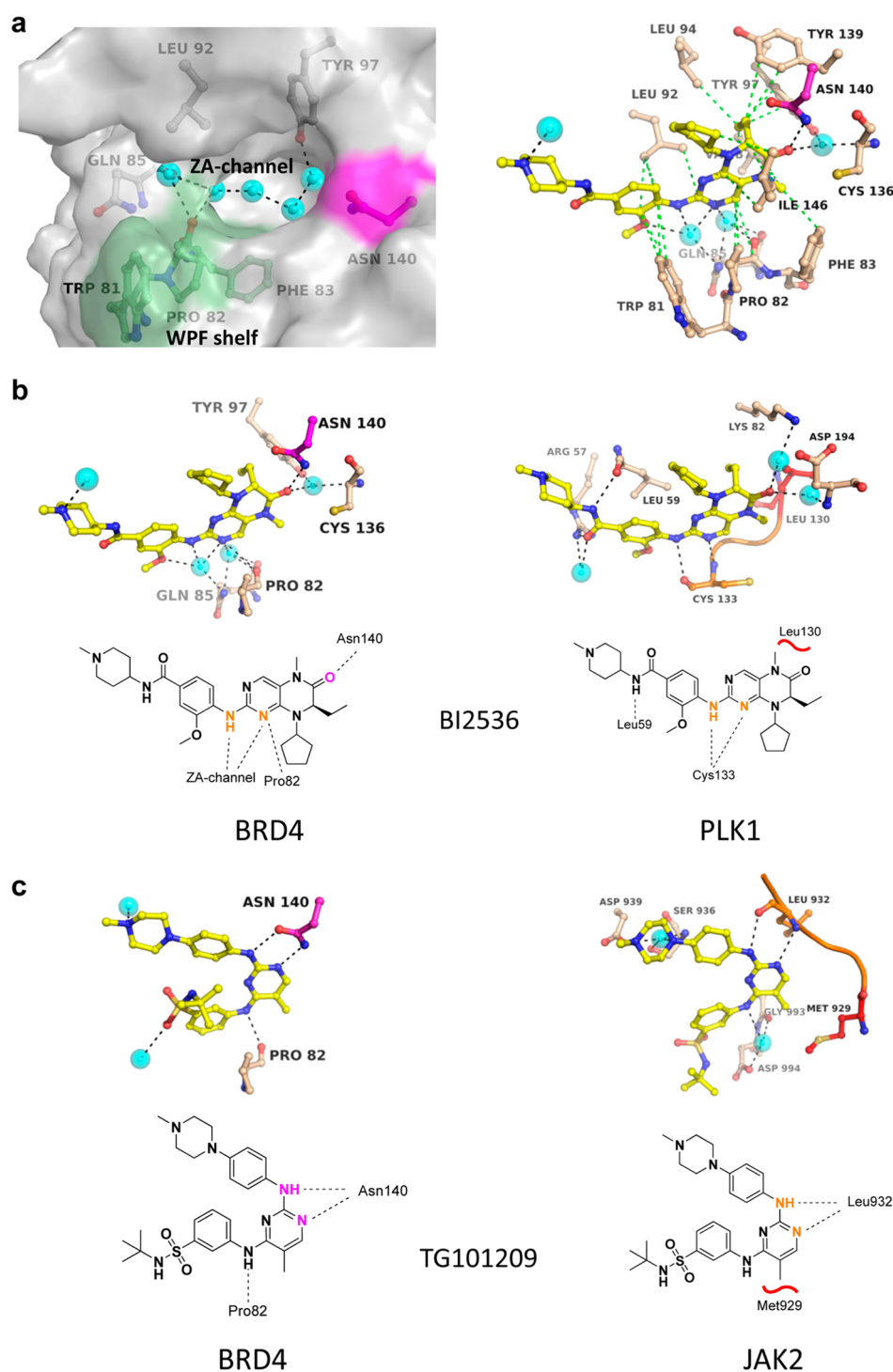
**Figure 3.** Differential binding modes of BI2536 and TG101209 in BRD4 and kinases. (A) General architecture of the KAc site in BRD4-1. The ZA channel consists of a network of tightly bound water molecules (cyan spheres) from Glu85 to Tyr97. The WPF shelf (green) constitutes one flank of the binding cleft opposite to Leu92. Asn140 is colored in magenta. The right panel shows the potential hydrogen bonding (black dotted lines) and VDW interactions (green dotted lines) of BI2536 in the KAc site of BRD4. (B) Hydrogen bonding interactions of BI2536 in BRD4 (left) and in PLK1 (right, PDB 2RKU) along with schematic presentations of the binding modes. Atoms colored in magenta interact with Asn140, and those colored in orange interact with the hinge region. The gatekeeper residue is indicated in red. (C) Hydrogen bonding interactions of TG101209 in BRD4 (left) and JAK2 (right, PDB 4JI9). Stereo presentations of the binding interactions of all identified BRD4 inhibitors are shown in Supplementary Figure S1.

dihydropteridine moiety (Figure 3B). The carbonyl oxygen interacts with Asn140 and the aminopyrimidine moiety interacts with Pro82 and water molecules of the ZA channel. As known potent inhibitors of BRD4 interact predominantly

with Asn140 (e.g., through triazole or isoxazole moieties), it is likely that the high affinity of BI2536 toward BRD4 results primarily from interaction of the dihydropteridine oxygen with Asn140, while additional hydrogen bonds with Pro82 and the
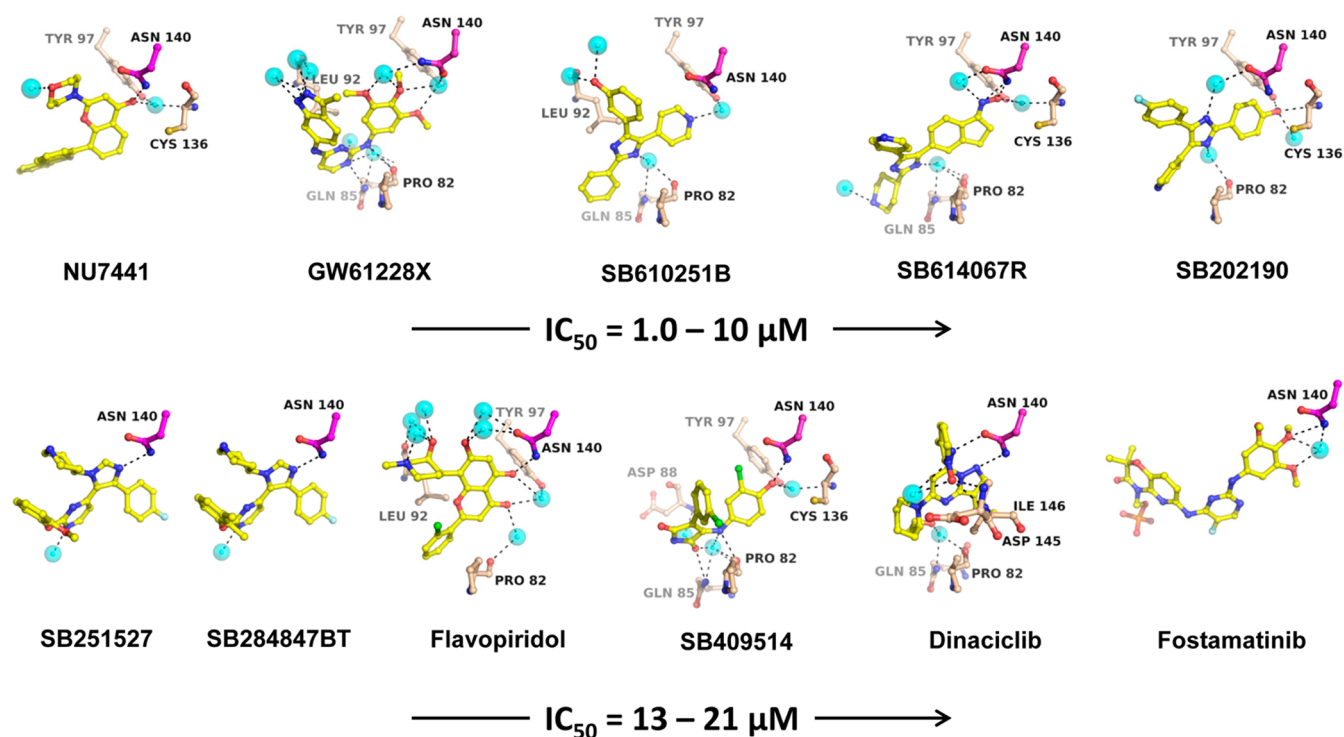
**Figure 4.** Hydrogen bonding interactions of kinase inhibitors in BRD4-1 with micromolar inhibitory activities. The color code is the same as in Figure 3.

ZA-channel stabilize the complex. In PLK1, BI2536 binds to the hinge region through the aminopyrimidine moiety while the dihydropteridine oxygen is involved in water-mediated interactions around the gatekeeper residue Leu130 (Figure 3B). Thus, the hinge-binding part of this kinase inhibitor is directed toward Pro82 and the ZA channel in BRD4.

The next strongest inhibitors of BRD4 and BRDT were the JAK2 inhibitors TG101209 and TG101348 (Selleck library) with $IC_{50}$ values between 130 and 340 nM. Recently, TG101348 treatment resulted in a significant decrease of disease burden in a phase III trial for patients with myelofibrosis.[29] TG101348 is also in several phase II studies for hematopoietic neoplasm (www.clinicaltrials.gov). TG101209 has yet to enter clinical trials; however, in a preclinical study it reduced tumor burden and promoted survival in a murine model of acute myeloid leukemia.[30] In contrast to BI2536, both JAK2 inhibitors utilize the hinge-binding aminopyrimidine moiety to directly interact with Asn140, while the opposite amino group interacts with Pro82 (Figure 3C). The different binding modes of BI2536 and TG101209 to BRD4 suggest that the KAc site provides two principal anchor points for hinge-binding groups of kinase inhibitors: Asn140 and Pro82/ZA-channel.
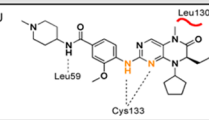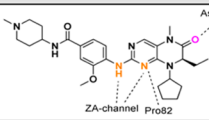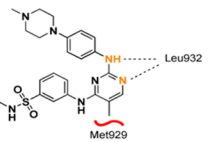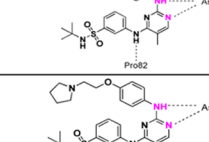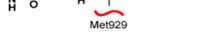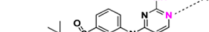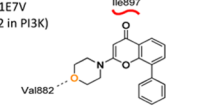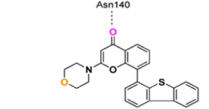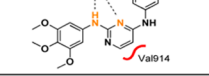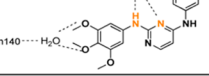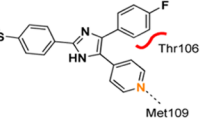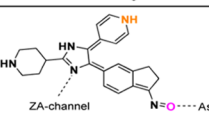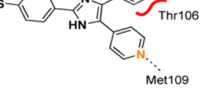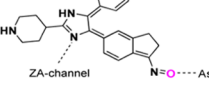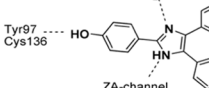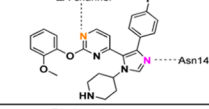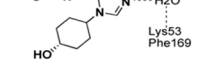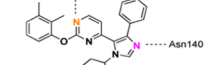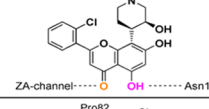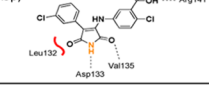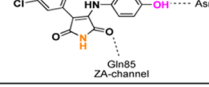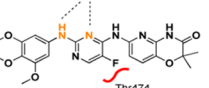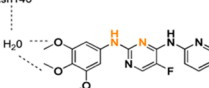
Five ligands were modest BET inhibitors with $IC_{50}$ values between 1 and 10 $\mu$M against BRD4 and similar values against BRDT; six ligands were weak inhibitors with $IC_{50}$ values above 10 $\mu$M (Figure 4). Analysis of all BRD4-ligand complexes and comparison with available kinase-inhibitor complexes suggests four general binding modes of kinase inhibitors to the KAc site (Table 1). Depending on the interactions established by the respective hinge-binding groups, the inhibitors were classified as Type N (interacting with Asn140; two scaffolds/three compounds), Type PZA (interacting with Pro82 and ZA channel; two scaffolds/two compounds), Type ZA (interacting

with ZA channel only; two scaffolds/three compounds), and Type I (not involved; four scaffolds/six compounds).

NU7441 (Selleck library) is a modest inhibitor of BRD4 and BRDT ($IC_{50}$ = 1 and 3.5 $\mu$M, respectively), which establishes a single hydrogen bond in the KAc site through the chromenone oxygen with Asn140 (Figure 4, Table 1). NU7441 is a potent and selective inhibitor of DNA-dependent protein kinase (DNA-PK) with an $IC_{50}$ of 14 nM,[31] and has been demonstrated to potentiate the cytotoxicity of ionizing radiation and chemotherapeutic drugs against cancer cell lines and a murine SW620 xenograft tumor model.[32] A crystal structure of NU7441 bound to a kinase is not available, but the structure of a close analogue, LY294002, bound to PI3K is known in which the morpholino oxygen of LY294002 interacts with the hinge region and the chromenone oxygen is in the vicinity of the gatekeeper residue with no apparent hydrogen bonding interactions (Table 1).[33] As the hinge-binding group of NU7441 is solvent-exposed in BRD4, this inhibitor can be classified as a Type I BRD inhibitor. Notably, LY294002 was recently identified as a modest inhibitor of BET bromodomains, and its binding mode in BRD4 is similar to that of NU7441.[34]

GW612286X (PKIS-I library) contains a scaffold highly similar to that of Pazopanib, a methoxy aniline-containing pyrimidine and potent pan-VEGFR inhibitor ($IC_{50}$ of 10, 37, and 47 nM against VEGFR-1, -2, and -3, respectively). Pazopanib is in clinical development as an oral treatment for renal cell cancer and other solid tumors.[35] GW612286X is a modest inhibitor of BRD4 and BRDT with $IC_{50}$ values of 4.6 and 7.6 $\mu$M, respectively (Figure 2). The aminopyrimidine moiety interacts with Pro82 and the ZA-channel, and the trimethoxyphenyl moiety appears to establish water-mediated hydrogen bonding interactions with Asn140 (Figure 4, Table 1). The principal binding mode of this inhibitor is similar to

**Table 1. Comparative Structural Analysis and Classification of Identified BRD4-Kinase Inhibitors**

| Compound ID (kinase target) | Main H-bonding interactions in kinase[a] | Main H-bonding interactions in BRD4-1[a] | Inhibitor Type[b] | PDB ID BRD4-1 |
|---|---|---|---|---|
| BI2536 (PLK1) | PDB: 2RKU (PLK1) | | PZA | 4O74 |
| TG101209 (JAK2, RET, FLT3) | PDB: 4JI9 (JAK2) | | N | 4O76 |
| TG101348 (JAK2) | | | N | 4O73 |
| NU7441 (DNA PK, PI3K) | PDB: 1E7V (LY294002 in PI3K) | | I | 4O72 |
| GW612286X (pan-kinase) | PDB: 3CJF (VEGFR2) | | PZA | 4O78 |
| SB610251B (p38α, HDR, RET, SRC) | PDB: 3ZS5 (SB2 in p38α) | | I | 4O7E |
| SB614067R (BRAF, p38α, LOK) | | | I | 4O7C |
| SB202190 (p38α, p38β) | | | I | 4O77 |
| SB251527 (p38α, p38β) | PDB: 4FA2 (SB239063 in p38α) | | ZA | 4O7F |
| SB284847BT (p38α, p38β) | | | ZA | 4O7B |
| Flavopiridol (CDKs) | PDB: 3BLR (CDK9) | | ZA | 4O71 |
| SB409514 (GSKα, GSKβ) | PDB: 1Q4L (I-5 in GSK3β) | | I | 4O7A |
| Dinaciclib (CDK1/2/5/9) | PDB: 4KD1 (CDK2) | | N | 4O70 |
| Fostamatinib (Syk, BTK) | PDB: 3PIY (BTK) | | I | 4O75 |

[a]Compounds ranked according to inhibitory potential (Figure 2). Color code: orange = hinge-binding groups; red wiggly line = location of the gatekeeper residue; magenta = interaction with Asn140 in BRD4. [b]Interaction of hinge-binding groups in BRD4: N = Asn140; PZA and ZA = Pro82 and/or ZA channel; I = not involved.

1165

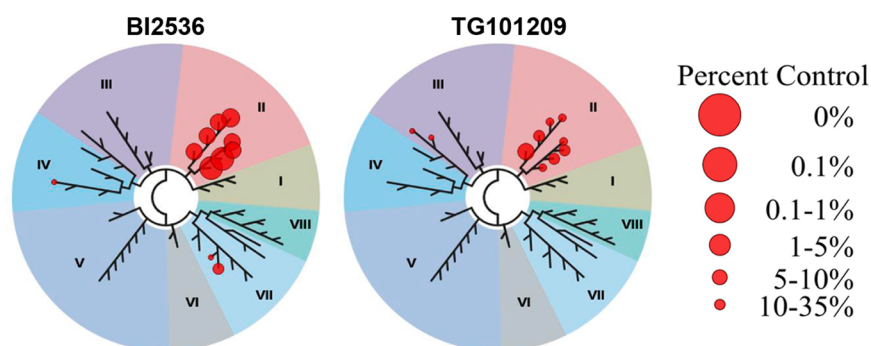dx.doi.org/10.1021/cb500072z | ACS Chem. Biol. 2014, 9, 1160−1171

**Figure 5.** Profiling of BI2536 and TG101209 against a panel of 32 human BRDs. The binding potential of BI2536 and TG101209 toward other human BRDs was determined in duplicate at a single compound concentration of 2 $\mu$M using a qPCR-based binding assay by Discoverx Corp. Binding activity is expressed as a percentage of the positive control, with lower values indicating higher binding affinity (larger circles). Shown is an artistic representation of the human BRD phylogenetic tree highlighting the potency and selectivity of these kinase inhibitors against BET BRDs (Family II). The other BRDs affected were TAF1L bromodomain 2 (TAF1L-2) and TAF1 bromodomain 2 (TAF1-2) (Family VII), and CREBBP and EP300 (Family III). The experimental values against each BRD are shown in Supplementary Table S3.

that of BI2536 (Type PZA), and the reduced potency is presumably due to the lack of direct interaction potential with Asn140.

Compounds SB610251B, SB614067R, and SB202190 (PKIS-I library) share the same imidazole-pyridine scaffold as SB203580,[36] an inhibitor of p38$\alpha$/$\beta$ (IC$_{50}$ of 0.3−0.5 $\mu$M). Animal studies have shown that SB203580 improves renal function in a murine model of systemic lupus erythematosus (SLE).[37] The imidazole-pyridine compounds identified in this study inhibit BRD4 with IC$_{50}$ values between 2.5 and 10 $\mu$M, predominantly through interactions of the imidazole ring with the ZA channel. Remarkably, each compound binds to the KAc site in a different orientation (Figure 4, Table 1). Although SB614067R appears to interact with Asn140 through its nitro group, it is the weakest inhibitor in this series, presumably caused by steric hindrance. Notably, SB202190 interacts with Tyr97 and Cys136, two residues not involved in binding interactions with any other inhibitor. As SB202190 displayed higher inhibitory activity and increased complex stability than the other two compounds of this series, these additional hydrogen bonds seem to favor binding potential. Crystal structures of these inhibitors bound to a kinase are not available, but comparison with SB203580 in p38$\alpha$ shows that the pyridine ring interacts with the hinge region.[36] Since the pyridine ring does not contribute to significant binding interactions in BRD4, this inhibitor series can be classified as Type I.

Compounds SB251527 and SB284847BT (PKIS-I library) contain imidazole-pyrimidine scaffolds highly similar to that of SB239063, also an inhibitor of p38$\alpha$ MAPK (IC$_{50}$ of 44 nM).[38] Preclinical studies have demonstrated that SB239063 reduces microglial activation and brain inflammation and restores normal brain function in rats with minimal hepatic encephalopathy (MHE).[39] SB251527 and SB284847BT interact with BRD4 in a markedly different manner from the above-described imidazole-pyridine inhibitors of p38$\alpha$ (Figure 4, Table 1). The imidazole moiety interacts with Asn140 while the pyrimidine ring interacts with the ZA channel. Crystal structures of these inhibitors in complex with a kinase are not available; however, the binding mode of SB239063 in p38$\alpha$ suggests that the pyrimidine interacts with the hinge region. Therefore, these compounds can be classified as Type ZA inhibitors.

Flavopiridol (Selleck library) was originally developed as a CDK2-selective inhibitor and was the first CDK inhibitor to

enter clinical trials.[40] It has been extensively studied in several phase I and II trials for the treatment of various cancers and is currently in phase II for relapsed/refractory lymphoma or multiple myeloma. Flavopiridol binds to the KAc site of BRD4 through interaction of the chromenone hydroxyl with Asn140 and the carbonyl oxygen with the ZA-channel. In CDK9, the hinge-binding group is the carbonyl oxygen, which classifies this compound as a Type ZA inhibitor.

SB409514 (PKIS-I library) is an inhibitor of GSK-3$\alpha$/$\beta$. It shares a 3-anilino-4-arylmaleimide scaffold with reportedly selective GSK-3$\alpha$/$\beta$ inhibitors such as I-5 (IC$_{50}$ = 160 nM).[41] SB409514 binds to BRD4 through interactions between the hydroxyl group of the 3-chloro-hydroxyaniline moiety and Asn140, the aniline NH group, and Pro82, and one of the oxygen atoms of the maleimide moiety with Gln85 and the ZA-channel (Figure 4, Table 1). In GSK3$\beta$, the NH group of the maleimide of compound I-5 interacts with the hinge region, and therefore this inhibitor scaffold appears to bind to BRD4 independent of the hinge-binding group (Type I).

Dinaciclib (Selleck library) is a new-generation highly potent inhibitor of CDKs with selectivity for CDK1, CDK2, CDK5, and CDK9 that recently advanced to phase III clinical trials for refractory chronic lymphocytic leukemia.[42] On the basis of our previously determined crystal structure of the BRDT-dinaciclib complex,[24] we expected that the binding mode of dinaciclib to BRDT was representative for BETs in general. However, the co-crystal structure of BRD4 in complex with dinaciclib revealed a markedly different binding mode (Supplementary Figure S4). In BRDT, the hinge-binding pyrazolo-pyrimidine moiety of dinaciclib binds to the ZA channel through two highly coordinated and structurally conserved water molecules, while the pyridine oxide interacts with the conserved Asn residue (Type ZA). By contrast, in BRD4 the pyrazolo-pyrimidine moiety binds to Asn140, and the pyridine oxide interacts with the main chain atoms of Asp145 and Ile146 (Type N, Table 1). Importantly, dinaciclib binding to BRDT induces a conformational change in the WPF shelf, which is not observed in the BRD4-dinaciclib complex or other BET-inhibitor complexes.

Fostamatinib, a prodrug of the active metabolite R406, is a poorly selective inhibitor of SYK (IC$_{50}$ of 41 nM).[43] To date, there have been 33 clinical trials in which fostamatinib has been tested for efficacy against a variety of conditions, including most recently in a phase II study for patients with solid tumors.[44]

Fostamatinib is a weak inhibitor of BRD4 and BRDT (IC$_{50}$ > 20 $\mu$M) and binds to BRD4 predominantly through van der Waals (VDW) hydrophobic interactions (Figure 4, Table 1). Similar to compound GW612286X, the trimethoxyphenyl moiety of fostamatinib appears to establish water-mediated interactions with Asn140. In SYK, the phosphate-free inhibitor interacts with the hinge region through the aminopyrimidine moiety, which is not involved in binding interactions with BRD4.

**Profiling of BI2536 and TG101209 against BRDs.** To assess inhibitory potential against BRDs other than BRD4-1 and BRDT-1, the most potent compounds, BI2536 and TG101209, were profiled against a panel of 32 human BRDs using a qPCR-based binding assay (Figure 5). As expected from the high structural similarity of the KAc sites in BET proteins, both compounds showed high selectivity for BRDs of the BET family, with BI2536 being the stronger inhibitor. Outside the BET family, BI2536 displayed appreciable activity against TAF1-2 and TAF1L-2, and TG101209 was modestly active against CREBBP and EP300 (Supplementary Table S3). Both compounds showed weak activities (30−42%) against BRPF1. Thus, BI2536 and TG101209 are highly selective for BET BRDs.

**Discussion.** This study combines the screening and validation of compound libraries in a single experimental setup using robotic co-crystallization followed by structure determination of crystals able to grow in the presence of compound. While this method is not suitable for high-throughput screening campaigns using large compound libraries, the value added through immediate confirmation of hit compounds by structure determination outweighs this shortcoming. Furthermore, co-crystallization screening allows the identification of weak binders, such as fostamatinib (provided they are soluble at 1 mM in 10% DMSO), which are otherwise typically discarded during HTS campaigns or remain undetected due to limited assay sensitivity. A weak inhibitor unambiguously identified as a ligand of BRD4 by crystallography may well serve as a starting point for the rational design of high-potency BET inhibitors, as has been demonstrated for numerous hit-to-lead development campaigns in kinase drug discovery. Our current hit rate of 7.2% (14 compounds from 194 crystal structures determined) suggests that other kinase inhibitors with potential as BET inhibitors remain to be discovered.

A comparative analysis of the binding interactions of these 14 hit compounds in BRD4 suggests that the KAc site is highly susceptible to inhibition by diverse kinase inhibitor scaffolds. Importantly, the hinge-binding groups can adopt different functions in the KAc site, interacting either with Asn140, Pro82 or water molecules of the ZA channel. Four of the 10 scaffolds bind to BRD4 independent of the respective hinge-binding moieties. Thus, each of the three most potent kinase inhibitor scaffolds (BI2536, TG101209/TG101348, and NU7441) interacts uniquely with the KAc site. The binding modes of BI2536 and TG101209 suggest that the concomitant interaction of kinase inhibitors with both Asn140 and Pro82 provides highest binding potential. However, hydrogen bonding potential alone does not explain the relatively weak activity of compounds that also establish multiple interactions in the KAc site, such as dinaciclib. Several regions of the KAc site are important to ensure shape complementarity and optimal positioning of inhibitors. Each inhibitor establishes multiple potential VDW interactions with hydrophobic residues

of the KAc site, particularly residues of the WPF shelf and Leu92, which are oppositely located in the binding cleft (Supplementary Figure S1). These interactions contribute to binding potential, but the WPF shelf also imposes significant steric hindrance for most kinase inhibitors (Figure 3A). As a result, most compounds assume slightly or notably different conformations in the KAc site as compared to the ATP site. Assuming that the binding modes in the respective ATP sites reflect the low energy states of these kinase inhibitors, certain conformational changes may result in unfavorably high energy states and, consequently, reduced binding potential. Notably, the buried surface area of the different BRD4-inhibitor complexes did not correlate with inhibitory potency (Supplementary Table S5).

BRDT was less sensitive to most kinase inhibitors than BRD4 (Figure 2). Although the KAc sites of BET proteins are highly conserved (Supplementary Table S4), subtle structural differences may influence shape complementarity between binding site and ligand. For example, Gln85 in BRD4 interacts with the main chain of Trp81, potentially stabilizing the WPF shelf (Supplementary Figure S4), whereas the equivalent residue in BRDT-1, Arg54, is solvent-exposed and not involved in interactions with other residues. As the WPF shelf of BRDT undergoes structural changes upon binding of dinaciclib, other kinase inhibitors may cause similar effects. The differential binding potential of kinase inhibitors toward BRD4 and BRDT indicates promise for the design of intra-BET selective inhibitors. Profiling against 32 BRDs revealed high selectivity of TG101209 and BI2536 for BET BRDs with moderate activities against CREBBP and EP300 (TG101209) and TAF1 and TAF1L (BI2536). Sequence alignment shows that Phe83, Tyr97, and Asn140 are highly conserved, whereas Trp81 and Pro82 of the WPF shelf vary among the BRDs (Supplementary Table S4). Outside of the BET BRD family, CREBBP and EP300 share the most highly conserved KAc sites with BRD4. Similarly, the KAc sites of TAF1-2 and TAF1L-2 are also well-conserved, with the critical asparagine and WPF shelf remaining intact. Conversely, most of the other human BRDs contain disrupted WPF shelves, seemingly contributing to the lack of inhibitory activity of TG101209 and BI2536 against these proteins. However, the WPF shelf is also conserved in CECR2, FALZ, GCN5L2, and PCAF, which are insensitive to either inhibitor. In these BRDs, Gln85 and Leu92 are replaced by Glu and Ser/Asn, respectively, indicating a significant role of these residues in inhibitor binding.

The 10 different scaffolds identified as KAc site binders provide new frameworks for the structure-based design of next-generation BET inhibitors. Depending on the binding type in the KAc site, compounds may be tailored as BET-specific or dual-activity kinase-BET inhibitors. Compounds such as NU7441 interact with the KAc site independently of the hinge-binding moiety (Type I) and therefore could be readily transformed into kinase-inactive inhibitors. Certain scaffolds in which the hinge-binding moiety interacts with Pro82 and/or the ZA-channel (types PZA or ZA) may tolerate slight modifications to decrease kinase inhibitory potential, whereas compounds in which the hinge-binding moiety directly interacts with Asn140 (type N) are dual BET-kinase inhibitors a priori. None of the kinase inhibitors disrupted the ZA water channel network but rather utilized these water molecules for hydrogen-bonding interactions. Addition of functional groups to displace water molecules by directly interacting with residues of the ZA channel may increase the binding potential of certain

inhibitors. Table 1 provides information for each scaffold with respect to the ZA channel, some of which may be suitable for the synthesis of analogues to probe the ZA channel in structure−activity relationship studies.

Combined, our results suggest that BET proteins are potential off-targets of diverse kinase inhibitors, the knowledge of which could significantly impact current practice in academic and clinical research. Many of the inhibitors identified are routinely used as chemical probes in biological studies, and some have advanced to clinical trials. Kinase inhibitors such as BI2536 and TG101209/TG101348 are likely to inhibit the intended kinase target and BET proteins simultaneously and effectively at relatively low concentrations (<2 $\mu$M, Figure 5). For cell lines sensitive to BET inhibitors such as JQ1, the use of kinase inhibitors to probe signaling pathways could lead to erroneous conclusions if the concomitant inhibition of BET proteins contributes to the cellular phenotype. Intriguingly, a recent report describes that the transcriptional changes induced by the BET inhibitor I-BET-151 and TG101209 in human erythroleukemic HEL cells are significantly overlapping, and it was concluded that these inhibitors have a common pathway of action.[45] Our findings indicate that these effects may be the result of simultaneous inhibition of JAK2 and BETs by TG101209 (dual pathway of action). The simultaneous inhibition of two structurally and functionally unrelated proteins by a single drug may prove beneficial in the treatment of medical conditions in which the interference with transcriptional (BET) and cell signaling (kinase) events is achieved through combination therapy using at least two drugs.

## ■ METHODS

Reagents and compounds for biochemical and crystallographic experiments were purchased from Sigma-Aldrich and Hampton Research unless otherwise indicated. The L1200 kinase inhibitor library was purchased from Selleck Chemicals, and the GSK Published Kinase Inhibitor Set 1 (PKIS-1) was kindly provided by Dr. David Drewry (GlaxoSmithKline). Protein concentration was determined by $A_{280}$ molar absorbance using a Nanodrop ND-1000 spectrophotometer (Nanodrop Technologies).

**Protein Purification.** The gene encoding the first bromodomain of human BRD4 (BRD4-1; residues 44−168) cloned in-frame with an N-terminal His$_6$ tag was received in a pNIC28-Bsa4 vector from Addgene (plasmid 38942).[2] Plasmid 38942 was subsequently transformed into competent E.coli strain BL21 (DE3) cells for protein expression. Bacterial cultures were grown for 2−3 h at 37 °C until $OD_{600}$ = 0.6, and then the temperature was decreased to 16 °C prior to induction with 0.1 mM IPTG. Cultures were grown for an additional 18 h at 16 °C, and then harvested by centrifugation (6,000 × g for 15 min at 4 °C). All protein purification steps were performed by fast protein liquid chromatography (FPLC) at 4 °C. Harvested bacterial pellets were resuspended in 50 mM Na/K phosphate buffer (pH 7.4) containing 100 mM NaCl, 10 mM imidazole, 0.5 mg mL$^{-1}$ lysosyme, and 0.01% Triton X-100 at 4 °C for 1 h. After sonication (30 s pulses on ice repeated for a total of three times) and centrifugation (30,000 × g for 45 min at 4 °C), the supernatant was purified by immobilized Ni$^{2+}$-ion affinity chromatography (GE LifeSciences). Following incubation of peak fractions with His-TEV protease (20:1) at 4 °C, the cleaved His tag was removed by a second Ni$^{2+}$-ion affinity column. BRD4-1 peak fractions were loaded on to a Superdex 75 (26/60) column and eluted with 10 mM HEPES buffer (pH 7.5) containing 100 mM NaCl and 1 mM DTT. Purified BRD4-1 was concentrated to 25 mg mL$^{-1}$ for crystallization studies and stored at −80 °C. The gene encoding the first bromodomain of human BRDT (BRDT-1; residues 21−137) cloned in-frame with an N-terminal His$_6$ tag was received in a pNIC28-Bsa4 vector from Addgene (plasmid 38898)[2] and purified as described previously.[24]

**Differential Scanning Fluorimetry (DSF).** The inhibitory activities of compounds against BRD4-1 and BRDT-1 were assessed by DSF using a StepOnePlus Real-Time PCR system (Applied Biosystems). Purified BRD4-1 (4 $\mu$M final concentration; 10 mM HEPES (pH 7.5), 100 mM NaCl, and 1 mM DTT), and BRDT-1 (4 $\mu$M final concentration; 50 mM phosphate (pH 7.4), 100 mM NaCl, and 1 mM DTT) were assayed, in quadruplicates, in a 96-well plate. Inhibitors were added to a final concentration of 100 $\mu$M and 2% DMSO. Protein Thermal Shift Dye (1:8000; Applied Biosystems) was used as the fluorescent probe, and fluorescence was measured using the ROX Reporter channel (620 nm). Protein stability was investigated by programing the thermocycler to increase the temperature from 25 to 99 °C using 0.2 °C increments and 10 s incubations per increment. The inflection point of the transition curve/melting temperature ($T_m$) was calculated using the Boltzmann equation within the Protein Thermal Shift Software (v.1.1) (Applied Biosystems). JQ1(+)[3] and dinaciclib[24] were used as controls for strong and weak binders of BRD4-1, respectively. The $\Delta T_m$ was calculated by using DMSO control wells as a reference.

**Compound Screening and Structure Determination.** Protein crystallization was performed with the mosquito LCP (TTP Labtech) crystallization robot at 18 °C using the sitting drop vapor diffusion method. The crystallization robot was programmed to (i) dispense 450 nL of BRD4-1 per triplicate subwell of a 96-well microplate (Corning); (ii) add 450 nL of reservoir (0.2 M (NH$_4$)$_2$SO$_4$, 0.1 M Tris (pH 8.5), and 25% (w/v) PEG 3350; (iii) add 100 nL of ligand (10 mM in DMSO) or DMSO; and (iv) mix two times using a mixing volume of 500 nL. Crystals of BRD4-1 were grown in the presence of 1 mM ligand and 10% (v/v) DMSO from reservoir, harvested in cryoprotectant (reservoir containing 25% (v/v) ethylene glycol and 0.5 mM ligand), and flash frozen in a stream of nitrogen gas. X-ray diffraction data for the BRD4-NU7441 crystal were recorded at −180 °C in the Moffitt Cancer Center Structural Biology Core using CuK$\alpha$ X-rays generated by a Rigaku Micro-Max 007-HF X-ray generator, focused by mirror optics and equipped with a Rigaku CCD Saturn 944 system. Data sets for all other crystals were collected at −180 °C using stations 22-ID and 22-BM, SER-CAT, Advanced Photon Source, Argonne National Laboratories. Data were reduced with HKL2000[46] or XDS,[47] and the resolution cutoff was applied using the following criteria for the highest resolution shell: completeness ≥ 90%, I/sI ≥ 3, redundancy ≥ 2, Rsym ≤ 35%. PHENIX[48] was employed for phasing and refinement, and model building was performed using Coot.[49] All structures were solved by molecular replacement using Phaser[50] and the monomer of PDB entry 2OSS[2] as the search model. Initial models for the small molecule ligands were generated using MarvinSketch (ChemAxon) with ligand restraints from eLBOW of the PHENIX suite. All structures were refined using simulated annealing and individual anisotropic B-value refinement on protein and ligand atoms. Fully refined structures were validated by MolProbity[51] and phenix.model_vs_data[52] before deposition in the PDB. Figures were prepared using PyMOL (Schrödinger).

**Alpha Screen Assay.** The half maximal inhibitory concentration (IC$_{50}$) of each compound against BRD4-1 and BRDT-1 was determined by Reaction Biology Corp. using the chemiluminescent Alpha Screen binding assay. Briefly, donor beads coated with streptavidin were incubated with biotinylated histone H4 peptide (residues 1−21) containing KAc (K5/8/12/16Ac). In the absence of inhibitor, His-tagged BRD binds to KAc-histone H4 peptide, thereby recruiting acceptor beads coated with a nickel chelator. Binding potential is assessed by detecting light emission (520−620 nm) from acceptor beads following laser excitation (680 nm) of a photosensitizer within the donor beads that converts ambient oxygen to singlet oxygen.

**Bromodomain Profiling.** The profiling of BI2536 and TG101209 against a panel of 32 BRDs was performed by Discoverx Corp. at a single compound concentration of 2 $\mu$M. The amount of BRD captured on an immobilized ligand in the presence or absence of compound was measured using a quantitative real-time polymerase chain reaction (qPCR) method that detects the associated DNA label tagged to the BRD. The results are reported as

$$\% \text{ of control}$$
$$= \frac{\text{inhibitor signal} - \text{positive control signal}}{\text{negative control signal (DMSO)} - \text{positive control signal}}$$

## ■ ASSOCIATED CONTENT

**Ⓢ Supporting Information**

This material is available free of charge via the Internet at http://pubs.acs.org.

**Accession Codes**

Atomic coordinates and structure factors for 14 BRD4-kinase inhibitor complexes have been deposited to the Protein Data Bank with accession codes 4O70, 4O71, 4O72, 4O73, 4O74, 4O75, 4O76, 4O77, 4O78, 4O7A, 4O7B, 4O7C, 4O7E, 4O7F.

## ■ AUTHOR INFORMATION

**Corresponding Author**

*E-mail: ernst.schonbrunn@moffitt.org.

**Author Contributions**

#These authors contributed equally to this work.

**Notes**

The authors declare no competing financial interest.

## ■ ACKNOWLEDGMENTS

## ■ REFERENCES

(1) Sanchez, R., and Zhou, M. M. (2009) The role of human bromodomains in chromatin biology and gene transcription. *Curr. Opin. Drug Discovery Dev. 12*, 659−665.

(2) Filippakopoulos, P., Picaud, S., Mangos, M., Keates, T., Lambert, J. P., Barsyte-Lovejoy, D., Felletar, I., Volkmer, R., Muller, S., Pawson, T., Gingras, A. C., Arrowsmith, C. H., and Knapp, S. (2012) Histone recognition and large-scale structural analysis of the human bromodomain family. *Cell 149*, 214−231.

(3) Filippakopoulos, P., Qi, J., Picaud, S., Shen, Y., Smith, W. B., Fedorov, O., Morse, E. M., Keates, T., Hickman, T. T., Felletar, I., Philpott, M., Munro, S., McKeown, M. R., Wang, Y., Christie, A. L., West, N., Cameron, M. J., Schwartz, B., Heightman, T. D., La Thangue, N., French, C. A., Wiest, O., Kung, A. L., Knapp, S., and Bradner, J. E. (2010) Selective inhibition of BET bromodomains. *Nature 468*, 1067−1073.

(4) French, C. A., Miyoshi, I., Kubonishi, I., Grier, H. E., Perez-Atayde, A. R., and Fletcher, J. A. (2003) BRD4-NUT fusion oncogene: a novel mechanism in aggressive carcinoma. *Cancer Res. 63*, 304−307.

(5) Darnell, J. E. (2002) Transcription factors as targets for cancer therapy. *Nat. Rev. Cancer 2*, 740−749.

(6) Dey, A., Chitsaz, F., Abbasi, A., Misteli, T., and Ozato, K. (2003) The double bromodomain protein Brd4 binds to acetylated chromatin during interphase and mitosis. *Proc. Natl. Acad. Sci. U.S.A. 100*, 8758−8763.

(7) Devaiah, B. N., and Singer, D. S. (2013) Two faces of brd4: mitotic bookmark and transcriptional lynchpin. *Transcription 4*, 13−17.

(8) Wang, R., Li, Q., Helfer, C. M., Jiao, J., and You, J. (2012) Bromodomain protein Brd4 associated with acetylated chromatin is important for maintenance of higher-order chromatin structure. *J. Chem. Biol. 287*, 10738−10752.

(9) Krueger, B. J., Varzavand, K., Cooper, J. J., and Price, D. H. (2010) The mechanism of release of P-TEFb and HEXIM1 from the 7SK snRNP by viral and cellular activators includes a conformational change in 7SK. *PLoS One 5*, e12335.

(10) Rahman, S., Sowa, M. E., Ottinger, M., Smith, J. A., Shi, Y., Harper, J. W., and Howley, P. M. (2011) The Brd4 extraterminal domain confers transcription activation independent of pTEFb by recruiting multiple proteins, including NSD3. *Mol. Cell. Biol. 31*, 2641−2652.

(11) Devaiah, B. N., Lewis, B. A., Cherman, N., Hewitt, M. C., Albrecht, B. K., Robey, P. G., Ozato, K., Sims, R. J., 3rd, and Singer, D. S. (2012) BRD4 is an atypical kinase that phosphorylates serine2 of the RNA polymerase II carboxy-terminal domain. *Proc. Natl. Acad. Sci. U.S.A. 109*, 6927−6932.

(12) Huang, B., Yang, X. D., Zhou, M. M., Ozato, K., and Chen, L. F. (2009) Brd4 coactivates transcriptional activation of NF-kappaB via specific binding to acetylated RelA. *Mol. Cell. Biol. 29*, 1375−1387.

(13) Shang, E., Salazar, G., Crowley, T. E., Wang, X., Lopez, R. A., Wang, X., and Wolgemuth, D. J. (2004) Identification of unique, differentiation stage-specific patterns of expression of the bromodomain-containing genes Brd2, Brd3, Brd4, and Brdt in the mouse testis. *Gene Expression Patterns 4*, 513−519.

(14) Shang, E., Nickerson, H. D., Wen, D., Wang, X., and Wolgemuth, D. J. (2007) The first bromodomain of Brdt, a testis-specific member of the BET sub-family of double-bromodomain-containing proteins, is essential for male germ cell differentiation. *Development 134*, 3507−3515.

(15) Gaucher, J., Boussouar, F., Montellier, E., Curtet, S., Buchou, T., Bertrand, S., Hery, P., Jounier, S., Depaux, A., Vitte, A. L., Guardiola, P., Pernet, K., Debernardi, A., Lopez, F., Holota, H., Imbert, J., Wolgemuth, D. J., Gérard, M., Rousseaux, S., and Khochbin, S. (2012) Bromodomain-dependent stage-specific male genome programming by Brdt. *EMBO J. 31*, 3809−3820.

(16) Jones, M. H., Numata, M., and Shimane, M. (1997) Identification and characterization of BRDT: A testis-specific gene related to the bromodomain genes RING3 and Drosophila fsh. *Genomics 45*, 529−534.

(17) Matzuk, M. M., McKeown, M. R., Filippakopoulos, P., Li, Q., Ma, L., Agno, J. E., Lemieux, M. E., Picaud, S., Yu, R. N., Qi, J., Knapp, S., and Bradner, J. E. (2012) Small-molecule inhibition of BRDT for male contraception. *Cell 150*, 673−684.

(18) Delmore, J. E., Issa, G. C., Lemieux, M. E., Rahl, P. B., Shi, J., Jacobs, H. M., Kastritis, E., Gilpatrick, T., Paranal, R. M., Qi, J., Chesi, M., Schinzel, A. C., McKeown, M. R., Heffernan, T. P., Vakoc, C. R., Bergsagel, P. L., Ghobrial, I. M., Richardson, P. G., Young, R. A., Hahn, W. C., Anderson, K. C., Kung, A. L., Bradner, J. E., and Mitsiades, C. S. (2011) BET bromodomain inhibition as a therapeutic strategy to target c-Myc. *Cell 146*, 904−917.

(19) Vollmuth, F., Blankenfeldt, W., and Geyer, M. (2009) Structures of the dual bromodomains of the P-TEFb-activating protein Brd4 at atomic resolution. *J. Biol. Chem. 284*, 36547−36556.

(20) Hewings, D. S., Rooney, T. P., Jennings, L. E., Hay, D. A., Schofield, C. J., Brennan, P. E., Knapp, S., and Conway, S. J. (2012) Progress in the development and application of small molecule inhibitors of bromodomain-acetyl-lysine interactions. *J. Med. Chem. 55*, 9393−9413.

(21) Mirguet, O., Gosmini, R., Toum, J., Clement, C. A., Barnathan, M., Brusq, J. M., Mordaunt, J. E., Grimes, R. M., Crowe, M., Pineau, O., Ajakane, M., Daugan, A., Jeffrey, P., Cutler, L., Haynes, A. C., Smithers, N. N., Chung, C. W., Bamborough, P., Uings, I. J., Lewis, A., Witherington, J., Parr, N., Prinjha, R. K., and Nicodeme, E. (2013) Discovery of epigenetic regulator I-BET762: lead optimization to afford a clinical candidate inhibitor of the BET bromodomains. *J. Med. Chem. 56*, 7501−7515.

(22) Seal, J., Lamotte, Y., Donche, F., Bouillot, A., Mirguet, O., Gellibert, F., Nicodeme, E., Krysa, G., Kirilovsky, J., Beinke, S., McCleary, S., Rioja, I., Bamborough, P., Chung, C.-W., Gordon, L., Lewis, T., Walker, A. L., Cutler, L., Lugo, D., Wilson, D. M., Witherington, J., Lee, K., and Prinjha, R. K. (2012) Identification of a novel series of BET family bromodomain inhibitors: binding mode and profile of I-BET151 (GSK1210151A). *Bioorg. Med. Chem. Lett. 22*, 2968–2972.

(23) Picaud, S., Da Costa, D., Thanasopoulou, A., Filippakopoulos, P., Fish, P. V., Philpott, M., Fedorov, O., Brennan, P., Bunnage, M. E., Owen, D. R., Bradner, J. E., Taniere, P., O'Sullivan, B., Muller, S., Schwaller, J., Stankovic, T., and Knapp, S. (2013) PFI-1, a highly selective protein interaction inhibitor, targeting BET Bromodomains. *Cancer Res. 73*, 3336–3346.

(24) Martin, M. P., Olesen, S. H., Georg, G. I., and Schonbrunn, E. (2013) Cyclin-dependent kinase inhibitor dinaciclib interacts with the acetyl-lysine recognition site of bromodomains. *ACS Chem. Biol. 8*, 2360–2365.

(25) Knapp, S., Arruda, P., Blagg, J., Burley, S., Drewry, D. H., Edwards, A., Fabbro, D., Gillespie, P., Gray, N. S., Kuster, B., Lackey, K. E., Mazzafera, P., Tomkinson, N. C., Willson, T. M., Workman, P., and Zuercher, W. J. (2013) A public-private partnership to unlock the untargeted kinome. *Nat. Chem. Biol. 9*, 3–6.

(26) Steegmaier, M., Hoffmann, M., Baum, A., Lenart, P., Petronczki, M., Krssak, M., Gurtler, U., Garin-Chesa, P., Lieb, S., Quant, J., Grauert, M., Adolf, G. R., Kraut, N., Peters, J. M., and Rettig, W. J. (2007) BI 2536, a potent and selective inhibitor of polo-like kinase 1, inhibits tumor growth in vivo. *Curr. Biol. 17*, 316–322.

(27) Muller-Tidow, C., Bug, G., Lubbert, M., Kramer, A., Krauter, J., Valent, P., Nachbaur, D., Berdel, W. E., Ottmann, O. G., Fritsch, H., Munzert, G., Garin-Chesa, P., Fleischer, F., Taube, T., and Dohner, H. (2013) A randomized, open-label, phase I/II trial to investigate the maximum tolerated dose of the Polo-like kinase inhibitor BI 2536 in elderly patients with refractory/relapsed acute myeloid leukaemia. *Br. J. Haematol. 163*, 214–222.

(28) Ellis, P. M., Chu, Q. S., Leighl, N., Laurie, S. A., Fritsch, H., Gaschler-Markefski, B., Gyorffy, S., and Munzert, G. (2013) A phase I open-label dose-escalation study of intravenous BI 2536 together with pemetrexed in previously treated patients with non-small-cell lung cancer. *Clin. Lung Cancer 14*, 19–27.

(29) Pardanani, A., Gotlib, J. R., Jamieson, C., Cortes, J. E., Talpaz, M., Stone, R. M., Silverman, M. H., Gilliland, D. G., Shorr, J., and Tefferi, A. (2011) Safety and efficacy of TG101348, a selective JAK2 inhibitor, in myelofibrosis. *J. Clin. Oncol. 29*, 789–796.

(30) Lo, M. C., Peterson, L. F., Yan, M., Cong, X., Hickman, J. H., Dekelver, R. C., Niewerth, D., and Zhang, D. E. (2013) JAK inhibitors suppress t(8;21) fusion protein-induced leukemia. *Leukemia 27*, 2272–2279.

(31) Leahy, J. J., Golding, B. T., Griffin, R. J., Hardcastle, I. R., Richardson, C., Rigoreau, L., and Smith, G. C. (2004) Identification of a highly potent and selective DNA-dependent protein kinase (DNA-PK) inhibitor (NU7441) by screening of chromenone libraries. *Bioorg. Med. Chem. Lett. 14*, 6083–6087.

(32) Zhao, Y., Thomas, H. D., Batey, M. A., Cowell, I. G., Richardson, C. J., Griffin, R. J., Calvert, A. H., Newell, D. R., Smith, G. C. M., and Curtin, N. J. (2006) Preclinical evaluation of a potent novel DNA-dependent protein kinase inhibitor NU7441. *Cancer Res. 66*, 5354–5362.

(33) Walker, E. H., Pacold, M. E., Perisic, O., Stephens, L., Hawkins, P. T., Wymann, M. P., and Williams, R. L. (2000) Structural determinants of phosphoinositide 3-kinase inhibition by wortmannin, LY294002, quercetin, myricetin, and staurosporine. *Mol. Cell 6*, 909–919.

(34) Dittmann, A., Werner, T., Chung, C.-W., Savitski, M. M., Fälth Savitski, M., Grandi, P., Hopf, C., Lindon, M., Neubauer, G., Prinjha, R. K., Bantscheff, M., and Drewes, G. (2013) The commonly used PI3-kinase probe LY294002 is an inhibitor of BET bromodomains. *ACS Chem. Biol. No. 9*, 495–502.

(35) Sternberg, C. N., Davis, I. D., Mardiak, J., Szczylik, C., Lee, E., Wagstaff, J., Barrios, C. H., Salman, P., Gladkov, O. A., Kavina, A., Zarba, J. J., Chen, M., McCann, L., Pandite, L., Roychowdhury, D. F., and Hawkins, R. E. (2010) Pazopanib in locally advanced or metastatic renal cell carcinoma: results of a randomized phase III trial. *J. Clin. Oncol. 28*, 1061–1068.

(36) Azevedo, R., Van Zeeland, M., Raaijmakers, H., Kazemier, B., de Vlieg, J., and Oubrie, A. (2012) X-ray structure of p38alpha bound to TAK-715: comparison with three classic inhibitors. *Acta Crystallogr., Sect. D: Biol. Crystallogr. 68*, 1041–1050.

(37) Jin, N., Wang, Q., Zhang, X., Jiang, D., Cheng, H., and Zhu, K. (2011) The selective p38 mitogen-activated protein kinase inhibitor, SB203580, improves renal disease in MRL/lpr mouse model of systemic lupus. *Int. Immunopharmacol. 11*, 1319–1326.

(38) Underwood, D. C., Osborn, R. R., Kotzer, C. J., Adams, J. L., Lee, J. C., Webb, E. F., Carpenter, D. C., Bochnowicz, S., Thomas, H. C., Hay, D. W., and Griswold, D. E. (2000) SB 239063, a potent p38 MAP kinase inhibitor, reduces inflammatory cytokine production, airways eosinophil infiltration, and persistence. *J. Pharmacol. Exp. Ther. 293*, 281–288.

(39) Agusti, A., Dziedzic, J. L., Hernandez-Rabaza, V., Guilarte, T. R., and Felipo, V. (2013) Rats with minimal hepatic encephalopathy due to portacaval shunt show differential increase of translocator protein (18 kDa) binding in different brain areas, which is not affected by chronic MAP-kinase p38 inhibition. *Metab. Brain Dis.*, DOI: 10.1007/s11011-013-9461-8.

(40) Senderowicz, A. M. (1999) Flavopiridol: the first cyclin-dependent kinase inhibitor in human clinical trials. *Invest. New Drugs 17*, 313–320.

(41) Smith, D. G., Buffet, M., Fenwick, A. E., Haigh, D., Ife, R. J., Saunders, M., Slingsby, B. P., Stacey, R., and Ward, R. W. (2001) 3-Anilino-4-arylmaleimides: potent and selective inhibitors of glycogen synthase kinase-3 (GSK-3). *Bioorg. Med. Chem. Lett. 11*, 635–639.

(42) Guha, M. (2012) Cyclin-dependent kinase inhibitors move into Phase III. *Nat. Rev. Drug Discovery 11*, 892–894.

(43) Braselmann, S., Taylor, V., Zhao, H., Wang, S., Sylvain, C., Baluom, M., Qu, K., Herlaar, E., Lau, A., Young, C., Wong, B. R., Lovell, S., Sun, T., Park, G., Argade, A., Jurcevic, S., Pine, P., Singh, R., Grossbard, E. B., Payan, D. G., and Masuda, E. S. (2006) R406, an orally available spleen tyrosine kinase inhibitor blocks fc receptor signaling and reduces immune complex-mediated inflammation. *J. Pharmacol. Exp. Ther. 319*, 998–1008.

(44) Park, S. R., Speranza, G., Piekarz, R., Wright, J. J., Kinders, R. J., Wang, L., Pfister, T., Trepel, J. B., Lee, M. J., Alarcon, S., Steinberg, S. M., Collins, J., Doroshow, J. H., and Kummar, S. (2013) A multi-histology trial of fostamatinib in patients with advanced colorectal, non-small cell lung, head and neck, thyroid, and renal cell carcinomas, and pheochromocytomas. *Cancer Chemother. Pharmacol. 71*, 981–990.

(45) Wyspianska, B. S., Bannister, A. J., Barbieri, I., Nangalia, J., Godfrey, A., Calero-Nieto, F. J., Robson, S., Rioja, I., Li, J., Wiese, M., Cannizzaro, E., Dawson, M. A., Huntly, B., Prinjha, R. K., Green, A. R., Gottgens, B., and Kouzarides, T. (2014) BET protein inhibition shows efficacy against JAK2V617F-driven neoplasms. *Leukemia 28*, 88–97.

(46) Otwinowski, Z., and Minor, W. (1997) Processing of X-ray diffraction data collected in oscillation mode. *Methods Enzymol. 276*, 307–326.

(47) Kabsch, W. (2010) Xds. *Acta Crystallogr., Sect. D: Biol. Crystallogr. 66*, 125–132.

(48) Adams, P. D., Afonine, P. V., Bunkoczi, G., Chen, V. B., Davis, I. W., Echols, N., Headd, J. J., Hung, L. W., Kapral, G. J., Grosse-Kunstleve, R. W., McCoy, A. J., Moriarty, N. W., Oeffner, R., Read, R. J., Richardson, D. C., Richardson, J. S., Terwilliger, T. C., and Zwart, P. H. (2010) PHENIX: a comprehensive Python-based system for macromolecular structure solution. *Acta Crystallogr., Sect. D: Biol. Crystallogr. 66*, 213–221.

(49) Emsley, P., Lohkamp, B., Scott, W. G., and Cowtan, K. (2010) Features and development of Coot. *Acta Crystallogr., Sect. D: Biol. Crystallogr. 66*, 486–501.

1170

dx.doi.org/10.1021/cb500072z | *ACS Chem. Biol.* 2014, 9, 1160–1171

(50) McCoy, A. J., Grosse-Kunstleve, R. W., Adams, P. D., Winn, M. D., Storoni, L. C., and Read, R. J. (2007) Phaser crystallographic software. *J. Appl. Crystallogr. 40*, 658−674.

(51) Chen, V. B., Arendall, W. B., Headd, J. J., Keedy, D. A., Immormino, R. M., Kapral, G. J., Murray, L. W., Richardson, J. S., and Richardson, D. C. (2010) MolProbity: all-atom structure validation for macromolecular crystallography. *Acta Crystallogr., Sect. D: Biol. Crystallogr. 66*, 12−21.

(52) Afonine, P. V., Grosse-Kunstleve, R. W., Chen, V. B., Headd, J. J., Moriarty, N. W., Richardson, J. S., Richardson, D. C., Urzhumtsev, A., Zwart, P. H., and Adams, P. D. (2010) phenix.model_vs_data: a high-level tool for the calculation of crystallographic model and data statistics. *J. Appl. Crystallogr. 43*, 669−676.